zation for Scientific Research (NWO). We thank Dr. S. Gambarotta for his valuable advice concerning the single-crystal sampling, A. J. M. Duisenberg for the data collection of **3**, and H. van der Heijden, Dr. E. J. M. de Boer, and Dr. C. J. Schaverien (Shell Research BV) for stimulating discussions.

Registry No. **2**, 122470-83-1; **3**, 122487-83-6.

Supplementary Material Available: ORTEP[39] drawings of **2** and **3** and tables of all atomic coordinates, thermal parameters, bond distances, bond angles, and torsion angles (28 pages); listings of observed and calculated structure factors (78 pages). Ordering information is given on any current masthead page.

Reactivity Studies of the Zirconium-Induced Insertion of Isonitriles into a 1-Sila-3-zirconacyclobutane Ring. Structural and Chemical Evidence of "Carbenium-Like" Intermediates for the Intramolecular 1,2-Silyl Shift and Reductive Coupling Reactions

Frederic J. Berg and Jeffrey L. Petersen*

Department of Chemistry, West Virginia University, Morgantown, West Virginia 26506-6045

Received May 15, 1989

The reaction of CNMe with $Cp^*_2Zr(CH_2SiMe_2CH_2)$ follows two different competitive pathways depending on the reaction conditions. At 25 °C, the lateral insertion of each equivalent of CNMe is accompanied by a 1,2-silyl shift and the stepwise formation of $Cp^*_2Zr(N(Me)C(=CH_2)SiMe_2CH_2)$ (**1**) and $Cp^*_2Zr(N(Me)C(=CH_2)SiMe_2(CH_2=)CN(Me))$ (**2**). Alternatively, upon repeating the reaction at −20 °C in the presence of excess CNMe, reductive coupling of two molecules of CNMe occurs with the formation of $Cp^*_2Zr(N(Me)C(CH_2SiMe_2CH_2)=CN(Me))$ (**3**). Structural and chemical evidence regarding the nature of the reactive intermediates involved in these intramolecular processes has been provided by an investigation of the reaction of *tert*-butyl isocyanide with $Cp_2Zr(CH_2SiMe_2CH_2)$ at 25 °C. Nucleophilic attack by the first equivalent of CN-*t*-Bu is accompanied by lateral insertion into a Zr–C bond and the formation of $Cp_2Zr(N(CMe_3)CCH_2SiMe_2CH_2)$ (**6**). The reaction of this η^2-iminoacyl species with a second equivalent of CN-*t*-Bu proceeds with reductive coupling of two molecules of CN-*t*-Bu and the formation of $Cp_2Zr(N(CMe_3)C—C(=NCMe_3)CH_2SiMe_2CH_2)$ (**7**) which upon thermolysis cleanly rearranges in solution to $Cp_2Zr(N(CMe_3)C(CH_2SiMe_2CH_2)=CN(CMe_3))$ (**8**). The molecular structures of **6** and **7** have been verified by X-ray diffraction methods. Crystal data for **6** at 25 °C: monoclinic space group $P2_1/n$ with a = 14.034 (3) Å, b = 15.550 (4) Å, c = 9.336 (2) Å, β = 93.14 (2)°, Z = 4. For **7** at 25 °C: monoclinic space group $P2_1/c$ with a = 8.422 (3) Å, b = 18.552 (5) Å, c = 16.318 (6) Å, β = 102.63 (3)°, Z = 4. The resulting structural information provides valuable insight into the nature of the "carbenium-like" intermediates involved in the intramolecular 1,2-silyl shift and reductive coupling reactions observed for 1-sila-3-zirconacyclobutane and related electrophilic complexes.

Introduction

Electron-deficient metal alkyl derivatives readily induce the migratory insertion of carbon monoxide into a metal–carbon bond.[1-14] The reactivity exhibited by the corresponding η^2-acyl complexes was initially attributed to an "oxycarbene" representation of the electronic structure

(1) (a) Bertolo, C. A.; Schwartz, J. *J. Am. Chem. Soc.* **1975**, *97*, 228. (b) Schwartz, J.; Labinger, J. A. *Angew. Chem., Int. Ed. Engl.* **1976**, *15*, 333.

(2) (a) Fachinetti, G.; Floriani, C.; Marchetti, F.; Merlino, S. *J. Chem. Soc., Chem. Commun.* **1976**, 522. (b) Fachinetti, G.; Fochi, G.; Floriani, C. *J. Chem. Soc., Dalton Trans.* **1977**, 1946. (c) Fachinetti, G.; Floriani, C.; Stoeckli-Evans, H. *J. Chem. Soc., Dalton Trans.* **1977**, 2297.

(3) Calderazzo, F. *Angew. Chem., Int. Ed. Engl.* **1977**, *16*, 299.

(4) (a) Manriquez, J. M.; McAlister, D. R.; Sanner, R. D.; Bercaw, J. E. *J. Am. Chem. Soc.* **1978**, *100*, 2716. (b) Wolczanski, P. T.; Bercaw, J. E. *Acc. Chem. Res.* **1980**, *13*, 121.

(5) (a) Manriquez, J. M.; Fagan, P. J.; Marks, T. J.; Day, C. S.; Day, V. W. *J. Am. Chem. Soc.* **1978**, *100*, 7112. (b) Fagan, P. J.; Manriquez, J. M.; Marks, T. J.; Day, V. W.; Vollmer, S. H.; Day, C. S. *J. Am. Chem. Soc.* **1980**, *102*, 5393. (c) Marks, T. J. *Science (Washington, D.C.)* **1982**, *217*, 989. (d) Sonnenberger, D. C.; Mintz, E. A.; Marks, T. J. *J. Am. Chem. Soc.* **1984**, *106*, 3484. (e) Moloy, K. G.; Marks, T. J. *J. Am. Chem. Soc.* **1984**, *106*, 7051. (f) Moloy, K. G.; Fagan, P. J.; Manriquez, J. M.; Marks, T. J. *J. Am. Chem. Soc.* **1986**, *108*, 56.

(6) (a) Erker, G.; Rosenfeldt, F. *Angew. Chem., Int. Ed. Engl.* **1978**, *17*, 605. (b) Erker, G.; Rosenfeldt, F. *J. Organomet. Chem.* **1980**, *188*, C1. (c) Erker, G.; Rosenfeldt, F. *J. Organomet. Chem.* **1982**, *224*, 29. (d) Erker, G. *Acc. Chem. Res.* **1984**, *17*, 103. (e) Erker, G.; Dorf, U.; Czisch, P.; Petersen, J. L. *Organometallics* **1986**, *5*, 668 and references cited therein.

(7) Marsella, J. A.; Moloy, K. G.; Caulton, K. G. *J. Organomet. Chem.* **1980**, *201*, 389.

(8) (a) Jeffery, J.; Lappert, M. F.; Luong-Thi, M. T.; Webb, M. *J. Chem. Soc., Dalton Trans.* **1981**, 1593. (b) Bristow, G. S.; Hitchcock, P. B.; Lappert, M. F. *J. Chem. Soc., Chem. Commun.* **1982**, 462. (c) Bristow, G. S.; Lappert, M. F.; Martin, T. R.; Atwood, J. L.; Hunter, W. F. *J. Chem. Soc., Dalton Trans.* **1984**, 399. (d) Lappert, M. F.; Raston, C. L.; Engelhardt, L. M.; White, A. H. *J. Chem. Soc., Chem. Commun.* **1985**, 521.

(9) Klei, E.; Teuben, J. H. *J. Organomet. Chem.* **1981**, *222*, 79.

(10) (a) Evans, W. J.; Wayda, A. L.; Hunter, W. E.; Atwood, J. L. *J. Chem. Soc., Chem. Commun.* **1981**, 706. (b) Evans, W. J. *Adv. Organomet. Chem.* **1985**, *24*, 131. (c) Evans, W. J.; Hughes, L. A.; Drummond, D. K.; Zhang, H.; Atwood, J. L. *J. Am. Chem. Soc.* **1986**, *108*, 1722.

(11) Engelhardt, L. M.; Jacobsen, G. E.; Raston, C. L.; White, A. H. *J. Chem. Soc., Chem. Commun.* **1984**, 220.

0276-7333/89/2308-2461$01.50/0

for the transition state.[4,5] However, on the basis of recent theoretical calculations, Hoffmann and co-workers[15] concluded that the electrophilicity of the acyl carbon atom in these and related complexes arises from the availability of a low-lying acceptor orbital. This alternative "carbenium-type" description accounts for several important bond forming reactions associated with CO activation. Specifically, intramolecular migration of a coor-

oxycarbene carbenium-type

dinated hydride[4,16] or an alkyl[17] /aryl[6b,18] ligand to an η^2-acyl proceeds with aldehyde or ketone formation, respectively. Similar intermolecular reactions have been employed in the preparation of bimetallic complexes containing bridging aldehyde[19] and ketone[20] linkages. In addition, intramolecular 1,2-hydride[5a,d] and 1,2-silyl[5a,d,8d,21,22] shifts to an η^2-acyl are important steps involved in enolate formation. Further evidence supporting this "carbenium-type" representation has been demonstrated dramatically by the intramolecular or intermolecular attack of phosphorus and nitrogen donors at the carbon of the η^2-acyl[23-25] or the related η^2-silaacyl[26] ligand.

Recent studies in our laboratory have revealed that the lateral insertion[27] of CO into one or both of the Zr–C bonds of the 1-sila-3-zirconacyclobutane ring of $Cp^*_2Zr(CH_2SiMe_2CH_2)$ ($Cp^* = \eta^5$-C_5Me_5) can follow two competitive reaction pathways.[28] At room temperature, the stepwise insertion of 2 equiv of CO proceeds with the sequential formation of a cyclic enolate, $Cp^*_2Zr(OC(=CH_2)SiMe_2CH_2)$, and a cyclic dienolate, $Cp^*_2Zr(OC(=CH_2)SiMe_2(CH_2=)CO)$. Each insertion step is accompanied by an intramolecular 1,2-silyl shift producing an exocyclic methylene group. Alternatively, when the carbonylation reaction is carried out at −78 °C with excess CO, reductive coupling of two carbonyls occurs with the formation of the bicyclic enediolate $Cp^*_2Zr(OC(CH_2SiMe_2CH_2)=CO)$.

Similar 1,2-silyl shift rearrangements have been observed in both cyclic[21,22] and acyclic[5a,d,8d] systems in which a silyl group occupies a β-position relative to an electron-deficient center. The characteristic ability of a Si atom to stabilize a positive charge at a β-carbon via hyperconjugation[29] presumably plays an important role in this intramolecular rearrangement. In light of Hoffmann's calculations,[15] one might envision that each 1,2-silyl shift could proceed via a Si-stabilized η^2-"carbenium-like" intermediate (eq 1).

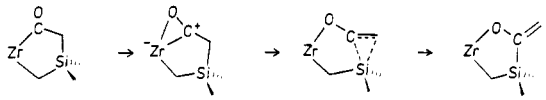

(1)

Further support for this proposed mechanism will require the isolation of a structurally similar η^2-intermediate, which exhibits reactivity compatible with the presence of an electrophilic carbon center.

With this in mind, an investigation of the reactivity of isonitriles with $Cp^*_2Zr(CH_2SiMe_2CH_2)$ and $Cp_2Zr(CH_2SiMe_2CH_2)$ was undertaken. The reactions of CNMe with these electron-deficient 1-sila-3-zirconacyclobutane complexes were carried out initially to determine the extent that methyl isocyanide mimics the insertion chemistry previously observed for CO. The replacement of Cp* by Cp further provides an opportunity to evaluate qualitatively the effect of increasing the electrophilicity of the zirconium on the CNMe insertion chemistry. Finally, since the coordination sphere around the zirconium in $Cp_2Zr(CH_2SiMe_2CH_2)$ is reasonably crowded, increasing the steric bulk of the alkyl substituent of the isocyanide may allow us to affect the course of the insertion chemistry by sterically preventing the occurrence of the 1,2-silyl shift. The reaction of *tert*-butyl isocyanide with $Cp_2Zr(CH_2SiMe_2CH_2)$ has provided an operational test of this premise and has led to the isolation of two unusual zirconadicyclic species, $Cp_2Zr(N(CMe_3)CCH_2SiMe_2CH_2)$ and $Cp_2Zr(N(CMe_3)C—C(=NCMe_3)CH_2SiMe_2CH_2)$, which are structurally and chemically compatible with a "carbenium-type" description for the η^2-iminoacyl group. The outcome of these experiments are described in detail and offer valuable insight into the nature of the reactive intermediates that are probably involved in the intramolecular 1,2-silyl shift and the reductive coupling reactions observed for CO and CNMe.

Experimental Section

General Considerations. All reactions and manipulations were carried out on a double-manifold, high-vacuum line and in a Vacuum Atmospheres glovebox. Nitrogen and argon were

(12) Young, S. J.; Hope, H.; Schore, N. E. *Organometallics* **1984**, *3*, 1585.
(13) Fanwick, P. E.; Kobriger, L. M.; McMullen, A. K.; Rothwell, I. P. *J. Am. Chem. Soc.* **1986**, *108*, 8095.
(14) Harrod, J. F.; Malek, A.; Rochon, F. D.; Melanson, R. *Organometallics* **1987**, *6*, 2117.
(15) Tatsumi, K.; Nakamura, A.; Hofmann, P.; Stauffert, P.; Hoffmann, R. *J. Am. Chem. Soc.* **1985**, *107*, 4440.
(16) Roddick, D. M.; Bercaw, J. E. *Chem. Ber.*, in press.
(17) Free ketone: (a) Fachinetti, G.; Floriani, C. *J. Chem. Soc., Chem. Commun.* **1972**, 654. (b) McDermott, J. X.; Wilson, M. E.; Whitesides, G. M.; *J. Am. Chem. Soc.* **1976**, *98*, 6529. (c) Hermes, A. R.; Girolami, G. S. *Organometallics* **1988**, *7*, 394. Coordinated ketone: (d) Wood, C. D.; Schrock, R. R. *J. Am. Chem. Soc.* **1979**, *101*, 5421. (e) Erker, G.; Czisch, P.; Schlund, R.; Angermund, K.; Krüger, C. *Angew. Chem., Int. Ed. Engl.* **1986**, *25*, 364.
(18) Stella, S.; Floriani, C. *J. Chem. Soc., Chem. Commun.* **1986**, *1053*.
(19) (a) Gell, K. I.; Williams, G. M.; Schwartz, J. *J. Chem. Soc., Chem. Commun.* **1980**, 550. (b) Threlkel, R. S.; Bercaw, J. E. *J. Am. Chem. Soc.* **1981**, *103*, 2650. (c) Marsella, J. A.; Folting, K.; Huffman, J. C.; Caulton, K. G. *J. Am. Chem. Soc.* **1981**, *103*, 5596. (d) Erker, G.; Kropp, K. *Chem. Ber.* **1982**, *115*, 2437. (e) Erker, G.; Kropp, K.; Krüger, C.; Chaing, A.-P. *Chem. Ber.* **1982**, *115*, 2447. (f) Gambarotta, S.; Floriani, C.; Chiesa-Villa, A.; Guastini, C. *J. Am. Chem. Soc.* **1983**, *105*, 1690. (g) Marsella, J. A.; Huffman, J. C.; Folting, K.; Caulton, K. G. *Inorg. Chim. Acta* **1985**, *96*, 161.
(20) (a) Martin, B. D.; Matchett, S. A.; Norton, J. R.; Anderson, O. P. *J. Am. Chem. Soc.* **1985**, *107*, 7952. (b) Waymouth, R. M.; Clauser, K. R.; Grubbs, R. H. *J. Am. Chem. Soc.* **1986**, *108*, 6385. (c) Waymouth, R. M.; Grubbs, R. H. *Organometallics* **1988**, *7*, 1631.
(21) (a) Simpson, S. J.; Andersen, R. A. *J. Am. Chem. Soc.* **1981**, *103*, 4063. (b) Planalp, R. P.; Andersen, R. A. *Organometallics* **1983**, *2*, 1675.
(22) Dormond, A.; Bouadili, A. A. E.; Moise, C. *J. Chem. Soc., Chem. Commun.* **1985**, 914.
(23) Labinger, J. A.; Bonfiglio, J. N.; Grimmett, D. L.; Masuo, S. T.; Shearin, E.; Miller, J. S. *Organometallics* **1983**, *2*, 733.
(24) Karsch, H. H.; Müller, G.; Krüger, C. *J. Organomet. Chem.* **1985**, *273*, 195.
(25) Bonnessen, P. V.; Yau, P. K. L.; Hersh, W. H. *Organometallics* **1987**, *6*, 1587.
(26) (a) Arnold, J.; Tilley, T. D.; Rheingold, A. L. *J. Am. Chem. Soc.* **1986**, *108*, 5355. (b) Arnold, J.; Tilley, T. D.; Rheingold, A. L. *J. Chem. Soc., Chem. Commun.* **1987**, 793. (c) Arnold, J.; Tilley, T. D.; Rheingold, A. L.; Geib, S. J. *Inorg. Chem.* **1987**, *26*, 2556. (d) Campion, B. K.; Falk, J.; Tilley, T. D. *J. Am. Chem. Soc.* **1987**, *109*, 2049. (e) Arnold, J.; Tilley, T. D.; Rheingold, A. L.; Geib, S. J.; Arif, A. T. *J. Am. Chem. Soc.* **1989**, *111*, 149.
(27) Lauher, J. W.; Hoffmann, R. *J. Am. Chem. Soc.* **1976**, *98*, 1729.
(28) Petersen, J. L.; Egan, J. W., Jr. *Organometallics* **1987**, *6*, 2007.
(29) Magnus, P. D.; Sarkar, T.; Djuric, S. In *Comprehensive Organometallic Chemistry*; Wilkinson, G., Stone, F. G. A., Abel, E. W., Eds.; Pergamon: Oxford, 1982; p 515.

prepurified by passage over reduced BTS catalysts and 4A molecular sieves. All glassware was thoroughly oven-dried or flame-dried under vacuum prior to use. Hydrocarbon and ethereal solvents (reagent grade) were purified by standard techniques[30] and distilled into storage flasks containing $[Cp_2Ti(\mu\text{-}Cl)_2]_2Zn$[31] prior to use. Hexamethyldisiloxane was distilled from $LiAlH_4$. Benzene-d_6 was vacuum distilled from 4A molecular sieves. CNMe was prepared by a literature method[32] and stored over 4A molecular sieves. *tert*-Butyl isocyanide (Aldrich) was dried over molecular sieves and distilled before use. $Cp_2Zr(CH_2SiMe_2CH_2)$[33] and $Cp^*_2Zr(CH_2SiMe_2CH_2)$[28] were prepared by using published procedures. A calibrated gas bulb equipped with high-vacuum Teflon stopcocks was used to control the quantitative addition of CNMe and CN-*t*-Bu. Elemental analyses of the reaction products were carried out by Dornis and Kolbe Microanalytical Laboratory, West Germany (DK), or Oneida Research Services, Whitesboro, NY (ORS).

^1H and ^{13}C spectra were recorded by using a JEOL GX-270 FT-NMR spectrometer operating in the FT mode at 270 (^1H) or 67.5 MHz (^{13}C). The ^1H chemical shifts are referenced to the residual proton peak of benzene-d_6 at δ 7.15 vs TMS, and the ^{13}C resonances are referenced to the central peak of benzene-d_6 at δ 128.0 vs TMS. IR spectra were measured on a Perkin-Elmer 1310 IR spectrometer using KBr disks or matched CaF_2 solution cells. The spectra were calibrated relative to polystyrene film. Electronic spectra were recorded on a Varian Cary-219 spectrometer using a 1.00-cm quartz cell equipped with a Teflon stopcock.

Synthesis of Compounds. Preparation of $Cp^*_2Zr(N(Me)C(=CH_2)SiMe_2CH_2)$ (1). In a typical reaction, 1.055 g (2.36 mmol) of $Cp^*_2Zr(CH_2SiMe_2CH_2)$ was added to a 100-mL solv-seal flask along with a stir bar. The flask was attached to a calibrated gas bulb, and ca. 50 mL of pentane was added via vacuum distillation. One equivalent of methyl isocyanide was added to the evacuated gas bulb. The stopcock separating the reaction flask from the bulb was opened for 15 s and then closed. This procedure was repeated three times at 1-h intervals. The stopcock was then left slightly open and the reaction stirred at room temperature for 5 days. The pentane was removed to yield a crude red product. The flask was then attached to a pressure equalizing filter frit and evacuated. Approximately 10 mL of diethyl ether was introduced, and the solution was filtered. Slow removal of the solvent from the reaction vessel that was cooled by an ice bath yielded red crystals of $Cp^*_2Zr(N(Me)C(=CH_2)SiMe_2CH_2)$ (76% isolated yield).

IR (KBr): 1535 (C=C stretch), 1155 cm^{-1} (C—N stretch). Anal. Calcd for $C_{26}H_{43}NSiZr$: C, 63.87; H, 8.86; N, 2.86. Found: C, 64.38; H, 8.27; N, 2.07 (ORS).

Preparation of $Cp^*_2Zr(N(Me)C(=CH_2)SiMe_2(CH_2=)CN(Me))$ (2). The procedure for 1 was repeated for a 0.574-g (1.28-mmol) sample of $Cp^*_2Zr(CH_2SiMe_2CH_2)$, and after 5 days a second equivalent of CNMe was added to the gas bulb. The stopcock on the bulb was left open slightly and the solution stirred another week. Volatiles were removed, and the crude red product was dried under vacuum overnight. Filtration of a pentane solution followed by slow removal of solvent gave a red microcrystalline product (80% isolated yield).

IR (KBr): 1560 (C=C stretch), 1175 cm^{-1} (C—N stretch).

Preparation of $Cp^*_2Zr(N(Me)C(CH_2SiMe_2CH_2)=CN(Me))$ (3). A 0.560-g (1.25-mmol) sample of $Cp^*_2Zr(CH_2SiMe_2CH_2)$ was added to a solv-seal flask. The flask was attached to a calibrated gas bulb and evacuated. Approximately 40 mL of pentane was condensed onto the solid and the solution warmed to −20 °C and stirred. To the evacuated gas bulb was added 4 equiv of methyl isocyanide. The isocyanide was then admitted into the flask and the yellow solution immediately turns dark purple upon mixing. The solution was stirred initially at −20 °C for 1 h and then at room temperature for 48 h. Following the removal of solvent the reaction flask was attached to a pressure equalizing filter frit and evacuated. Approximately 10 mL of diethyl ether was added via vacuum distillation, and the solution was warmed to room temperature and stirred. Decantation through the frit and slow removal of the solvent gave 0.630 g (95% isolated yielded) of a dark purple crystalline solid.

IR (KBr): 1550 (C=C stretch), 1192 cm^{-1} (C—N stretch). Anal. Calcd for $C_{28}H_{46}N_2SiZr$: C, 63.46; H, 8.75. Found: C, 62.71; H, 8.69 (DK).

Preparation of $Cp_2Zr(N(Me)C(=CH_2)SiMe_2CH_2)$ (4). A 0.405-g (1.32-mmol) sample of $Cp_2Zr(CH_2SiMe_2CH_2)$ was added to a 100-mL solv-seal flask and connected to a calibrated gas bulb. Pentane (40 mL) was condensed onto the solid. The solution was brought to −10 °C and stirred. One equivalent of CNMe was added in small increments over a period of 6–8 days. After the addition was complete, the reaction was stirred for an additional 24 h and the pentane was removed to yield a red, oily residue. Although many attempts were made to obtain this compound in a crystalline form, the product was always contaminated by a small amount of the dienamide **5**.

Preparation of $Cp_2Zr(N(Me)C(=CH_2)SiMe_2(CH_2=)CN(Me))$ (5). A 100-mL solv-seal flask charged with 0.808 g (2.63 mmol) of $Cp_2Zr(CH_2SiMe_2CH_2)$ was attached to a gas bulb and evacuated. Approximately 30 mL of pentane was added to the flask and warmed to room temperature. Two equivalents of methyl isocyanide were added to the evacuated bulb. The stopcock was opened and the solution stirred for at least 1 week. Removal of the solvent yielded a red solid. Recrystallization from an ether solution gave **5** as a light red powder (80% isolated yield).

IR (KBr): 1590 (C=C stretch), 1160 cm^{-1} (C—N stretch). Anal. Calcd for $C_{18}H_{26}N_2SiZr$: C, 55.47; H, 6.72; N, 7.19. Found: C, 55.94; H, 6.72; N, 6.95 (ORS).

Preparation of $Cp_2Zr(N(CMe_3)CCH_2SiMe_2CH_2)$ (6). A 0.823-g (2.68-mmol) sample of $Cp_2Zr(CH_2SiMe_2CH_2)$ was added to a solv-seal flask. Approximately 50 mL of pentane was added, and the gas bulb was charged with 1 equiv of CN-*t*-Bu. The solution was then frozen in liquid nitrogen, and the CN-*t*-Bu was condensed into the flask. The solution was brought to room temperature and stirred for 2 h. The color of the solution changed from light yellow to light orange as the reaction proceeded. The solvent was removed in vacuo leaving a light yellow crystalline product (88% isolated yield).

IR (KBr): 1625 cm^{-1}, medium (C=N stretch). Anal. Calcd for $C_{19}H_{29}NSiZr$: C, 58.40; H, 7.48. Found: C, 57.34; H, 7.50 (DK).

Crystals suitable for X-ray diffraction studies were obtained by the slow removal of hexamethyldisiloxane from a saturated solution.

Preparation of $Cp_2Zr(N(CMe_3)C—C(=NCMe_3)CH_2SiMe_2CH_2)$ (7). A freshly sublimed sample of $Cp_2Zr(CH_2SiMe_2CH_2)$ (0.416 g, 1.35 mmol) was added to a 100-mL solv-seal flask. Pentane (50 mL) was condensed onto the solid, and the gas bulb was charged with 2 equiv of CN-*t*-Bu. The solution was cooled to −70 °C, and the CN-*t*-Bu was admitted into the flask. After being warmed to room temperature, the reaction mixture was stirred for 5 days. The solvent was removed, and the light yellow crystalline product was dried in vacuo (90% isolated yield). Alternatively, **7** can be prepared by the addition of 1 equiv of CN-*t*-Bu to **6**.

IR (KBr): 1620, weak (C=N stretch); 1595 cm^{-1}, medium (C=N stretch). Anal. Calcd for $C_{24}H_{38}N_2SiZr$: C, 60.83; H, 8.08. Found: C, 60.05; H, 8.10 (DK).

Crystals suitable for X-ray diffraction studies were obtained by the slow removal of pentane or ether from a saturated solution.

All of the compounds have been characterized spectroscopically by ^1H and ^{13}C NMR methods. The NMR data are summarized in Table I.

(30) Gordon, A. J.; Ford, R. A. *The Chemist's Companion*; Wiley-Interscience: New York, 1972; pp 431–436.
(31) Sekutowski, D. G.; Stucky, G. D. *Inorg. Chem.* **1975**, *14*, 2192.
(32) Schuster, R. E.; Scott, J. E.; Casanova, J., Jr. *Org. Synth.* **1973**, *5*, 773.
(33) Tikkanen, W. R.; Liu, J. Z.; Egan, J. W., Jr.; Petersen, J. L. *Organometallics* **1984**, *3*, 825.

Table I. ^1H and ^{13}C NMR Data for Compounds 1–7

compound	^1H NMR		^{13}C NMR (mult, $^1J_{C-H}$ in Hz)	
$Cp^*_2Zr(N(Me)C(=CH_2)SiMe_2CH_2)$ (1)	$SiMe_2$	0.53 (s)	$SiCH_3$	4.74 (q, J = 118)
	$ZrCH_2$	1.27 (s)	C—CH_3	12.4 (q, J = 126)
	C—CH_3	1.79 (s)	N—CH_3	34.5 (q, J = 131)
	N—CH_3	2.17 (s)	Zr—CH_2	47.9 (t, J = 116)
	C=CH_2	4.01 (s)	C=CH_2	84.4 (dd, J = 151, 155)
		4.19 (s)	C—CH_3	120.2 (s)
			N—C=	164.9 (s)
$Cp^*_2Zr(N(Me)C(=CH_2)SiMe_2(CH_2=)CN(Me))$ (2)	$SiMe_2$	0.70 (s)	$SiCH_3$	3.42 (q, J = 119)
	C—CH_3	1.74 (s)	C—CH_3	12.2 (q, J = 126)
	N—CH_3	2.07 (s)	N—CH_3	31.2 (q, J = 133)
	C=CH_2	4.36 (s)	C=CH_2	89.1 (dd, J = 153, 155)
		4.53 (s)	C—CH_3	123.1 (s)
			N—C=	159.3 (s)
$Cp^*_2Zr(N(Me)C(CH_2SiMe_2CH_2)=CN(Me))$ (3)	$SiMe_2$	0.19 (s)	$SiCH_3$	−0.55 (q, J = 121)
	C—CH_3	1.88 (s)	C—CH_3	11.9 (q, J = 126)
	=C—CH_2	1.92 (s)	=C—CH_2	18.9 (t, J = 123)
	N—CH_3	3.31 (s)	N—CH_3	40.4 (q, J = 132)
			C—CH_3	116.2 (s)
			N—C	not observed
$Cp_2Zr(N(Me)C(=CH_2)SiMe_2CH_2)$ (4)	$SiMe_2$	0.40 (s)	$SiCH_3$	2.61 (q, J = 121)
	$ZrCH_2$	1.78 (s)	NCH_3	36.4 (q, J = 133)
	N—CH_3	2.22 (s)	$ZrCH_2$	42.7 (t, J = 120)
	C=CH_2	4.15 (s)	C=CH_2	86.6 (dd, J = 153, 158)
		4.24 (s)	C_5H_5	111.7 (d, J = 172)
	C_5H_5	5.81 (s)	C—N	not observed
$Cp_2Zr(N(Me)C(=CH_2)SiMe_2(CH_2=)CN(Me))$ (5)	$SiMe_2$	0.42 (s)	$SiCH_3$	−0.45 (q, J = 119)
	NCH_3	2.54 (s)	NCH_3	39.5 (q, J = 133)
	C=CH_2	4.54 (s)	C=CH_2	94.0 (dd, J = 152, 158)
		4.58 (s)	C_5H_5	112.7 (d, J = 172)
	C_5H_5	5.84 (s)	C—N	not observed
$Cp_2Zr(N(CMe_3)CCH_2SiMe_2CH_2)$ (6)	$ZrCH_2$	−0.11 (s)	$SiCH_3$	2.3 (q, J = 118)
	$SiMe_2$	0.19 (s)	$ZrCH_2$	5.8 (t, J = 113)
	$NCMe_3$	1.07 (s)	$NC(CH_3)_3$	29.7 (q, J = 126)
	CCH_2Si	2.51 (s)	CCH_2Si	32.7 (t, J = 125)
	C_5H_5	5.50 (s)	$NCMe_3$	58.4 (s)
			C_5H_5	106.6 (d, J = 170)
			Zr—CN	232.5 (s)
$Cp_2Zr(N(CMe_3)C—C(=NCMe_3)CH_2SiMe_2CH_2)$ (7)	$ZrCH_2$	−0.44 (s)	$ZrCH_2$	3.9 (t, J = 112)
	$SiMe_2$	0.35 (s)	$SiCH_3$	4.3 (q, J = 118)
	$NCMe_3$	1.33 (s)	$NC(CH_3)_3$	29.7 (q, J = 125)
		1.37 (s)		31.1 (q, J = 125)
	CCH_2Si	1.92 (s)	CCH_2Si	34.2 (t, J = 122)
	C_5H_5	5.52 (s)	$NCMe_3$	55.7 (s)
				61.4 (s)
			C_5H_5	107.5 (d, J = 171)
			C—CN	169.3 (s)
			$ZrCN$	228.9 (s)

X-ray Data Collection. The same general procedures were employed to collect the X-ray diffraction data for complexes **6** and **7**. Each crystal was sealed in a glass capillary tube under a prepurified N_2 atmosphere and then was transferred to a Picker goniostat which is operated by a Krisel Control diffractometer automation system. Following a preliminary analysis of low-angle reflections the orientation angles (ω, χ, and 2θ) for 20 higher order reflections were calculated and optimized by an automatic peak-centering routine[34] and least-squares fit to provide the corresponding refined lattice parameters (Table II) and the orientation matrix.

Intensity data ($\pm hkl$) were measured with Zr-filtered Mo Kα X-ray radiation at a takeoff angle of 2°. A θ–2θ scan mode was employed with a fixed scan rate and a variable scan width. The intensities of the three standard reflections were measured periodically. The integrated intensity, I, and its standard deviation, $\sigma_c(I)$, for each of the measured peaks were calculated from the expressions $I = w(S/t_s - B/t_b)$ and $\sigma_c(I) = w(S/t_s^2 + B/t_b^2)^{1/2}$, where S represents the total scan count measured in time t_s and B is the combined background count in time t_b. The intensity data were corrected for crystal decay, absorption, and Lorentz–polarization effects. The standard deviation of the square of each structure factor, $F_o^2 = I/Lp$, was calculated from $\sigma(F_o^2) = [\sigma_c(F_o^2)^2 + (pF_o^2)^2]^{1/2}$. Duplicate reflections were averaged. Specific details with regard to the lattice parameters and the data collection procedure are summarized in Table II.

Structural Analyses of 6 and 7. Initial coordinates for the zirconium atom in both compounds were obtained from an interpretation of the Harker vectors given by an unsharpened three-dimensional Patterson map. Approximate coordinates for the remaining non-hydrogen atoms were obtained from subsequent Fourier summations and were refined with anisotropic thermal parameters. All of the hydrogen atoms were located with difference Fourier techniques using only low-angle data with (sin θ)/λ < 0.40 Å^{-1}. Full matrix refinement (based on F_o^2)[35–39] of the

(34) The peak-centering algorithm is similar to that described by Busing: Busing, W. R. *Crystallographic Computing*; Ahmed, F. R, Ed.; Munksgaard: Copenhagen, 1970; p 319. The ω, χ, and 2θ angles were optimized with respect to the Kα_1 peak (λ = 0.709 26 Å).

(35) The least-squares refinement[36] of the X-ray diffraction data was based upon the minimization of $\sum\omega_i|F_o^2 - S^2F_c^2|^2$, where ω_i is the individual weighting factor and S is the scale factor. The discrepancy indices were calculated from the expressions: $R(F_o) = \sum||F_o| - |F_c||/\sum|F_o|$, $R(F_o^2) = \sum|F_o^2 - F_c^2|/\sum F_c^2$, and $R_w(F_o^2) = [\sum\omega_i|F_o^2 - F_c^2|^2/\sum\omega_i F_o^4]^{1/2}$. The standard deviation of an observation of unit weight, σ_1, equals $[\sum\omega_i|F_o^2 - F_c^2|/(n - p)]^{1/2}$, where n is the number of observations and p is the number of parameters varied during the last refinement cycle.

Table II. Data for the X-ray Diffraction Analyses of $Cp_2\overline{Zr(N(CMe_3)CCH_2SiMe_2CH_2)}$ (6) and $Cp_2\overline{Zr(N(CMe_3)C—C(=NCMe_3)CH_2SiMe_2CH_2)}$ (7)

	6	7
	A. Crystal Data	
cryst system	monoclinic	monoclinic
space group	$P2_1/n$	$P2_1/c$ (C_{2h}^5, No. 14)
a, Å	14.034 (3)	8.422 (3)
b, Å	15.550 (4)	18.552 (5)
c, Å	9.336 (2)	16.318 (6)
β, deg	93.14 (2)	102.63 (3)
V, Å^3	2034 (1)	2488 (1)
fw, amu	390.75	473.89
d_{calcd}, g/cm^3	1.276	1.265
Z	4	4
μ, cm^{-1}	5.87	4.94
	B. Data Collection and Analysis Summary	
cryst dimens, mm	0.15 × 0.25 × 0.50	0.25 × 0.325 × 0.75
reflctns sampled	$\pm hkl$ ($5° < 2\theta < 55°$)	$\pm hkl$ ($5° < 2\theta < 45°$)
2θ range for centered reflctns, deg	30–35	30–35
scan rate, deg/min; t_b, s	2; 20	4; 10
scan width, deg	1.1 + 0.8 tan θ	1.1 + 0.9 tan θ
no. of std reflctns	3	3
% cryst decay	11	1
total no. of measd reflctns	4480	3400
no. of unique data used	3069 ($F_o^2 > 2\sigma(F_o^2)$)	3258 ($F_o^2 > 0$)
agreement between equivalent data		
$R_{av}(F_o)$	0.020	0.033
$R_{av}(F_o^2)$	0.020	0.036
p	0.03	0.03
discrepancy indices for	3069 data with $F_o^2 > 2\sigma(F_o^2)$	2863 data with $F_o^2 > \sigma(F_o^2)$
$R(F_o)$	0.063	0.044
$R(F_o^2)$	0.056	0.055
$R_w(F_o^2)$	0.091	0.078
σ_1	1.69	1.66
no. of variables	315	367
data to parameter ratio	9.74:1	8.91:1

positional and anisotropic thermal parameters for the 22 non-hydrogen atoms and isotropic temperature factors for the 29 hydrogen atoms for complex **6** led to final discrepancy indices of $R(F_o) = 0.063$, $R(F_o^2) = 0.056$, and $R_w(F_o^2) = 0.091$ with $\sigma_1 = 1.69$ for the 3069 reflections with $F_o^2 > 2\sigma(F_o^2)$. A final difference map did not reveal any additional regions of significant electron density. The same refinement procedure for the 28 non-hydrogen atoms and 38 hydrogen atoms of complex **7** converged with final discrepancy indices of $R(F_o) = 0.044$, $R(F_o^2) = 0.055$, and $R_w(F_o^2) = 0.078$ with $\sigma_1 = 1.66$ for the 2863 reflections with $F_o^2 > \sigma(F_o^2)$. A final difference Fourier map was essentially featureless with no residuals of electron density of significant magnitude.

The positional parameters from the last least-squares refinement cycles are provided in Tables III and IV for **6** and **7**, respectively. Selected interatomic distances and bond angles and their estimated standard deviations (esd's) for the non-hydrogen atoms are given in Table V for **6** and Table VI for **7**. Tables of the thermal parameters, all of the non-hydrogen bond distances and angles, the equations for pertinent least-squares planes, and their dihedral angles and tables of the observed and calculated structure factors for **6** and **7** are available as supplementary material.[40]

(36) The scattering factors employed in all of the structure factor calculations were those of Cromer and Mann[37] for the non-hydrogen atoms and those of Stewart et al.[38] for the hydrogen atoms with corrections included for anomalous dispersion.[39]

(37) Cromer, D. T.; Mann, J. B. *Acta Crystallogr., Sect. A* **1968**, *A24*, 321.

(38) Stewart, R. F.; Davidson, E. R.; Simpson, W. T. *J. Chem. Phys.* **1965**, *42*, 3175.

(39) Cromer, D. T.; Liberman, D. *J. Chem. Phys.* **1970**, *53*, 1891.

(40) The computer programs that were used for the X-ray diffraction data analyses are described in: Nicholson, G. A.; Petersen, J. L.; McCormick, B. J. *Inorg. Chem.* **1980**, *19*, 195.

Table III. Positional Parameters for All of the Atoms in $Cp_2\overline{Zr(N(CMe_3)CCH_2SiMe_2CH_2)}$[a]

atom	x	y	z
Zr	0.12443 (3)	0.22929 (3)	0.03455 (4)
Si	0.27129 (9)	0.39997 (9)	−0.06216 (15)
N	0.1256 (2)	0.3195 (2)	0.2200 (3)
C1	0.2011 (3)	0.3285 (3)	0.1556 (4)
C2	0.2805 (4)	0.3901 (4)	0.1418 (6)
C3	0.2363 (4)	0.2914 (4)	−0.1204 (6)
C4	0.1831 (6)	0.4851 (5)	−0.1073 (10)
C5	0.3876 (6)	0.4386 (7)	−0.1259 (12)
C6	0.0915 (3)	0.3671 (3)	0.3460 (5)
C7	0.0678 (6)	0.4608 (5)	0.2958 (10)
C8	0.0035 (7)	0.3219 (7)	0.3912 (10)
C9	0.1706 (6)	0.3690 (6)	0.4627 (7)
C10	−0.0237 (5)	0.3168 (6)	−0.0409 (9)
C11	0.0206 (5)	0.3007 (5)	−0.1647 (8)
C12	0.0118 (5)	0.2148 (6)	−0.1883 (8)
C13	−0.0369 (5)	0.1778 (6)	−0.0812 (11)
C14	−0.0568 (4)	0.2407 (7)	0.0153 (9)
C15	0.2591 (7)	0.1415 (5)	0.1521 (13)
C16	0.1814 (9)	0.1255 (5)	0.2314 (10)
C17	0.1146 (6)	0.0825 (4)	0.1494 (10)
C18	0.1517 (6)	0.0694 (4)	0.0177 (9)
C19	0.2392 (6)	0.1052 (4)	0.0171 (12)
H1	0.279 (3)	0.447 (4)	0.200 (5)
H2	0.342 (4)	0.363 (3)	0.156 (5)
H3	0.285 (4)	0.259 (3)	−0.104 (5)
H4	0.217 (3)	0.287 (3)	−0.211 (6)
H5	0.207 (4)	0.539 (4)	−0.083 (6)
H6	0.120 (5)	0.476 (4)	−0.087 (7)
H7	0.171 (4)	0.495 (4)	−0.206 (7)
H8	0.382 (4)	0.444 (4)	−0.236 (7)
H9	0.431 (5)	0.409 (4)	−0.075 (7)
H10	0.403 (4)	0.497 (4)	−0.077 (7)
H11	0.044 (4)	0.487 (4)	0.374 (7)
H12	0.008 (4)	0.450 (4)	0.223 (6)
H13	0.132 (4)	0.483 (4)	0.254 (6)
H14	−0.044 (4)	0.321 (4)	0.301 (7)
H15	−0.020 (4)	0.342 (4)	0.480 (7)
H16	0.039 (4)	0.265 (4)	0.447 (7)
H17	0.143 (4)	0.400 (4)	0.533 (7)
H18	0.226 (4)	0.405 (4)	0.419 (6)
H19	0.182 (4)	0.306 (4)	0.486 (6)
H20	−0.020 (4)	0.365 (4)	−0.004 (6)
H21	0.051 (4)	0.348 (4)	−0.210 (6)
H22	0.041 (3)	0.192 (3)	−0.249 (5)
H23	−0.058 (5)	0.124 (4)	−0.080 (7)
H24	−0.091 (4)	0.239 (3)	0.120 (7)
H25	0.302 (5)	0.170 (5)	0.173 (8)
H26	0.174 (5)	0.141 (4)	0.319 (7)
H27	0.047 (4)	0.062 (4)	0.176 (7)
H28	0.117 (5)	0.042 (4)	−0.082 (7)
H29	0.276 (5)	0.109 (4)	−0.068 (8)

[a] The estimated standard deviations in parentheses for this and all subsequent tables refer to the least-significant figures.

Discussion of Results

Reactivity of CNMe with $Cp^*_2\overline{Zr(CH_2SiMe_2CH_2)}$. The controlled addition of CNMe to $Cp^*_2\overline{Zr(CH_2SiMe_2CH_2)}$ at room temperature proceeds with the stepwise insertion of 2 equiv of CNMe into the zirconium–carbon bonds of the 1-sila-3-zirconacyclobutane ring to produce a cyclic eneamide, **1**, and a cyclic dienamide, **2** (eq 2). The lateral insertion of each equivalent of CNMe

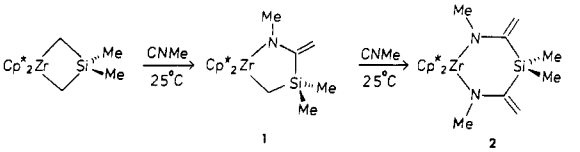

(2)

is accompanied by an intramolecular 1,2-silyl shift. This reaction sequence follows the same pathway observed for

Table IV. Positional Parameters for All of the Atoms in $Cp_2Zr(N(CMe_3)C{-}C(=NCMe_3)CH_2SiMe_2CH_2)$

atom	x	y	z
Zr	0.12818 (4)	0.08632 (2)	0.34646 (2)
Si	0.18930 (14)	−0.10679 (5)	0.33908 (7)
N1	0.2404 (3)	0.1023 (1)	0.2360 (2)
N2	0.2975 (4)	−0.0345 (2)	0.1399 (2)
C1	0.2475 (4)	0.0356 (2)	0.2527 (2)
C2	0.3141 (4)	−0.0296 (2)	0.2183 (2)
C3	0.3670 (5)	−0.0823 (2)	0.2890 (3)
C4	0.1544 (5)	−0.0314 (2)	0.4059 (2)
C5	0.0098 (6)	−0.1293 (3)	0.2550 (3)
C6	0.2532 (7)	−0.1923 (2)	0.3990 (3)
C7	0.2952 (4)	0.1461 (2)	0.1706 (2)
C8	0.4686 (6)	0.1263 (3)	0.1681 (4)
C9	0.1811 (6)	0.1319 (3)	0.0869 (3)
C10	0.2869 (7)	0.2251 (2)	0.1943 (4)
C11	0.3477 (5)	−0.0971 (2)	0.0949 (3)
C12	0.2989 (8)	−0.0775 (3)	0.0033 (3)
C13	0.2604 (8)	−0.1664 (3)	0.1091 (4)
C14	0.5336 (8)	−0.1060 (3)	0.1202 (4)
C15	−0.1276 (5)	0.0610 (3)	0.2353 (3)
C16	−0.1105 (5)	0.1349 (3)	0.2415 (3)
C17	−0.1325 (5)	0.1563 (2)	0.3186 (4)
C18	−0.1637 (5)	0.0940 (3)	0.3613 (3)
C19	−0.1608 (5)	0.0362 (3)	0.3088 (3)
C20	0.3884 (6)	0.1036 (3)	0.4590 (3)
C21	0.3796 (6)	0.1622 (3)	0.4073 (3)
C22	0.2469 (7)	0.2026 (2)	0.4139 (3)
C23	0.1762 (7)	0.1698 (3)	0.4739 (3)
C24	0.2625 (7)	0.1086 (3)	0.5004 (3)
H1	0.413 (5)	−0.122 (2)	0.273 (2)
H2	0.444 (5)	−0.060 (2)	0.335 (2)
H3	0.073 (5)	−0.043 (2)	0.430 (2)
H4	0.253 (5)	−0.031 (2)	0.456 (2)
H5	−0.018 (5)	−0.094 (2)	0.214 (3)
H6	−0.073 (5)	−0.133 (2)	0.278 (3)
H7	0.023 (4)	−0.171 (2)	0.224 (2)
H8	0.365 (4)	−0.184 (2)	0.447 (2)
H9	0.270 (5)	−0.226 (2)	0.363 (2)
H10	0.167 (5)	−0.209 (2)	0.413 (3)
H11	0.470 (5)	0.083 (2)	0.146 (3)
H12	0.505 (4)	0.165 (2)	0.129 (2)
H13	0.532 (5)	0.139 (2)	0.221 (3)
H14	0.179 (5)	0.083 (2)	0.071 (2)
H15	0.081 (5)	0.151 (2)	0.090 (2)
H16	0.221 (4)	0.158 (2)	0.045 (2)
H17	0.365 (4)	0.236 (2)	0.252 (2)
H18	0.192 (5)	0.233 (2)	0.200 (3)
H19	0.318 (4)	0.256 (2)	0.152 (2)
H20	0.347 (5)	−0.035 (2)	−0.010 (2)
H21	0.180 (5)	−0.062 (2)	−0.012 (2)
H22	0.329 (5)	−0.117 (2)	−0.031 (3)
H23	0.287 (5)	−0.203 (2)	0.076 (2)
H24	0.134 (5)	−0.154 (2)	0.088 (2)
H25	0.301 (4)	−0.183 (2)	0.171 (3)
H26	0.559 (5)	−0.126 (2)	0.175 (3)
H27	0.567 (5)	−0.139 (2)	0.082 (2)
H28	0.587 (5)	−0.061 (2)	0.107 (2)
H29	−0.126 (5)	0.035 (2)	0.194 (3)
H30	−0.089 (5)	0.160 (2)	0.201 (3)
H31	−0.123 (5)	0.199 (2)	0.336 (3)
H32	−0.175 (5)	0.097 (2)	0.414 (3)
H33	−0.175 (5)	−0.008 (2)	0.325 (2)
H34	0.463 (5)	0.068 (2)	0.465 (2)
H35	0.440 (5)	0.168 (2)	0.369 (2)
H36	0.216 (5)	0.240 (2)	0.391 (3)
H37	0.085 (5)	0.185 (2)	0.489 (2)
H38	0.244 (5)	0.076 (2)	0.535 (3)

the corresponding carbonylation reactions of $Cp^*_2Zr(CH_2SiMe_2CH_2)$.[28]

The enamides **1** and **2** were identified by ^1H and ^{13}C NMR measurements. The two magnetically inequivalent protons of the exocyclic methylene group appear as singlets at δ 4.01 and 4.19 for **1** and at δ 4.36 and 4.53 for **2**. In the

Table V. Selected Interatomic Separations (Å) and Bond Angles (deg) in $Cp_2Zr(N(CMe_3)CCH_2SiMe_2CH_2)$[a,b]

A. Interatomic Separations (Å)

Zr–N	2.227 (3)	Zr–C1	2.164 (4)
Zr–C3	2.396 (6)		
Zr–Cp(1)	2.277 (7)	Zr–Cp(2)	2.246 (8)
Si–C2	1.907 (5)	Si–C4	1.846 (8)
Si–C3	1.832 (6)	Si–C5	1.868 (9)
N–C1	1.255 (5)	N–C6	1.491 (6)
C1–C2	1.480 (7)	C6–C7	1.562 (9)
C6–C8	1.502 (11)	C6–C9	1.512 (9)

range of Zr–C (Cp rings): 2.522 (6)–2.582 (8)
range of C–C (Cp rings): 1.349 (11)–1.395 (16)

B. Bond Angles (deg)

N–Zr–C1	33.2 (1)	N–Zr–C3	103.8 (2)
C1–Zr–C3	72.8 (2)	Cp(1)–Zr–Cp(2)	128.2 (3)
Zr–N–C1	70.7 (2)	Zr–C1–N	76.2 (2)
Zr–N–C6	159.5 (3)	Zr–C1–C2	140.7 (4)
C6–N–C1	129.7 (4)	C2–C1–N	140.5 (3)
C1–C2–Si	97.4 (3)	Zr–C3–Si	111.5 (3)
C2–Si–C3	103.0 (3)	C3–Si–C4	115.3 (3)
C2–Si–C4	107.1 (3)	C3–Si–C5	115.3 (4)
C2–Si–C5	109.4 (4)	C4–Si–C5	106.5 (4)
N–C6–C7	107.4 (5)	C7–C6–C8	110.9 (6)
N–C6–C8	107.0 (5)	C7–C6–C9	109.5 (6)
N–C6–C9	108.9 (5)	C8–C6–C9	112.9 (6)

range of C–C–C (Cp rings): 106.0 (7)–110.0 (8)

[a] Cp(n) denotes the centroid of a cyclopentadienyl ring. [b] The esd's for the interatomic distances and bond angles were calculated from the standard errors for the fractional coordinates of the corresponding atomic positions.

Table VI. Selected Interatomic Separations (Å) and Bond Angles (deg) in $Cp_2Zr(N(CMe_3)C{-}C(=NCMe_3)CH_2SiMe_2CH_2)$[a,b]

A. Interatomic Separations (Å)

Zr–N1	2.231 (3)	Zr–C1	2.216 (4)
Zr–C4	2.378 (4)		
Zr–Cp(1)	2.237 (5)	Zr–Cp(2)	2.264 (6)
N1–C1	1.266 (4)	N2–C2	1.259 (5)
N1–C7	1.493 (5)	N2–C11	1.484 (5)
C1–C2	1.492 (5)	C2–C3	1.504 (5)
Si–C3	1.910 (5)	Si–C4	1.836 (4)
Si–C5	1.853 (5)	Si–C6	1.880 (5)
C7–C8	1.515 (6)	C11–C12	1.506 (7)
C7–C9	1.511 (6)	C11–C13	1.525 (7)
C7–C10	1.522 (6)	C11–C14	1.538 (8)

range of Zr–C (Cp rings): 2.506 (5)–2.555 (5)
range of C–C (Cp rings): 1.366 (8)–1.404 (8)

B. Bond Angles (deg)

N1–Zr–C1	33.1 (1)	N1–Zr–C4	115.7 (1)
C1–Zr–C4	82.9 (1)	Cp(1)–Zr–Cp(2)	129.9 (2)
Zr–N1–C1	72.8 (2)	Zr–C1–N1	74.1 (2)
Zr–N1–C7	154.5 (2)	Zr–C1–C2	150.2 (3)
C7–N1–C1	132.7 (3)	C2–C1–N1	135.6 (3)
C1–C2–C3	108.1 (3)	C1–C2–N2	118.3 (3)
C3–C2–N2	132.9 (3)	C2–N2–C11	125.4 (3)
C2–C3–Si	110.8 (3)	Zr–C4–Si	118.0 (2)
C3–Si–C4	108.3 (2)	C4–Si–C5	113.6 (2)
C3–Si–C5	109.0 (2)	C4–Si–C6	113.5 (2)
C3–Si–C6	105.2 (2)	C5–Si–C6	106.8 (2)
N1–C7–C8	109.8 (3)	N2–C11–C12	104.9 (4)
N1–C7–C9	108.5 (3)	N2–C11–C13	112.7 (4)
N1–C7–C10	107.7 (4)	N2–C11–C14	109.6 (3)
C8–C7–C9	111.2 (4)	C12–C11–C13	108.6 (4)
C8–C7–C10	109.7 (4)	C12–C11–C14	109.5 (5)
C9–C7–C10	110.0 (3)	C13–C11–C14	111.4 (4)

range of C–C–C (Cp rings): 107.1 (4)–108.8 (5)

[a] Cp(n) denotes the centroid of a cyclopentadienyl ring. [b] The esd's for the interatomic distances and bond angles were calculated from the standard errors for the fractional coordinates of the corresponding atomic positions.

gated nondecoupled ^{13}C NMR spectrum, the carbon resonance exhibits a characteristic resonance pattern consisting of a doublet of doublets at 85–95 ppm. For **1**, this doublet of doublets is centered at δ 84.4 with $^1J_{C-H}$ = 151 and 155 Hz, whereas for **2**, it is located at δ 89.1 with $^1J_{C-H}$ = 153 and 155 Hz. As expected, a low intensity singlet with no proton coupling is observed at δ 164.9 and 159.3 for the quaternary carbon(s) bound to the nitrogen and silicon atoms in **1** and **2**, respectively. The corresponding resonances for the hydrogen and carbon atoms of the methyl group(s) bound to the nitrogens, to the pentamethylcyclopentadienyl ring carbons, and to the silicon atoms are readily assignable. The carbon resonance of the remaining methylene group of the 1-aza-3-sila-5-zirconacyclopentane ring in **1** is observed as a triplet at δ 47.9 with $^1J_{C-H}$ = 116 Hz.

The infrared spectra of **1** and **2** exhibit a band at 1535 and at 1550 cm^{-1}, respectively, consistent with the presence of a carbon–carbon double bond. The corresponding carbon–nitrogen stretching bands at 1155 and at 1175 cm^{-1} are much too low for a carbon-nitrogen double or triple bond and thereby reflect the fact that CNMe has completely inserted into the zirconium–carbon bond(s) of the 1-sila-3-zirconacyclobutane ring.

The key to conducting this reaction at room temperature is that the first equivalent of CNMe must be added to $Cp^*_2Zr(CH_2SiMe_2CH_2)$ slowly in small increments. By keeping the concentration of CNMe low, the possible contamination of **1** by a small amount of **2** can be minimized. Fortunately, the relative rate of the first insertion is sufficiently faster to permit the isolation of **1** under these controlled reaction conditions. The manner by which the second equivalent of CNMe is added to **1** is less critical since only **2** is formed.

The reaction of CNMe with $Cp^*_2Zr(CH_2SiMe_2CH_2)$ was also performed at –20 °C by using an excess of CNMe. In this case, reductive coupling of two molecules of CNMe occurs leading to the formation of a dark purple compound, which on the basis of the ^1H and ^{13}C NMR data given in Table I is identified as the bicyclic enediamidate $Cp^*_2Zr(N(Me)C(CH_2SiMe_2CH_2)=CN(Me))$ (**3**) (eq 3). Simi-

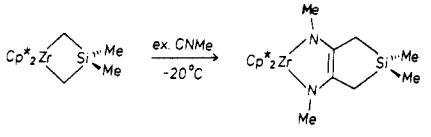

(3)

3

lar enediamino complexes have been obtained by the reductive coupling of isocyanides following insertion into either an electrophilic metal–hydride[41] or metal–carbon[42,43] bond. The unusual color of **3** is attributed to an electronic transition from the filled π-orbital of the carbon–carbon double bond to the empty dz^2-like orbital of the zirconium. For similar enediolate complexes, Hofmann and co-workers[44] observed that the energy of this transition increases as the folding of the ZrO_2C_2 ring along the O···O vector increases. The corresponding absorption maximum for **3** (λ_{max} = 546 nm) is comparable in energy to that of $Cp^*_2Zr(OC(CMe_3)=C(CMe_3)O)$, which possesses a planar structure for its five-membered chelate ring.[44]

Collectively, these results show that the reactions of CNMe with $Cp^*_2Zr(CH_2SiMe_2CH_2)$ completely mimic the corresponding insertion reactions observed for carbon monoxide. Two completely different reaction pathways are possible depending on the reaction conditions. At room temperature, each zirconium-induced insertion of CNMe is accompanied by an intramolecular 1,2-silyl shift (eq 2), whereas at low temperature an alternative reductive coupling reaction is observed (eq 3). Apparently, at –20 °C the activation barrier for the 1,2-silyl shift is sufficiently high that when CNMe is present in a large excess, the reductive coupling process predominates with **3** being the only observed product.

Insertion Reactions of CNMe with $Cp_2Zr(CH_2SiMe_2CH_2)$. The controlled addition of CNMe to $Cp_2Zr(CH_2SiMe_2CH_2)$ at ambient temperature sequentially affords the red enamide $Cp_2Zr(N(Me)C(=CH_2)SiMe_2CH_2)$ (**4**) and the dienamide $Cp_2Zr(N(Me)C(=CH_2)SiMe_2(CH_2=)CN(Me))$ (**5**) (eq 4). The lateral

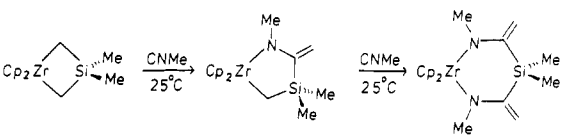

(4)

4 5

insertion of each CNMe is accompanied by an intramolecular 1,2-silyl shift. The reaction follows the same pathway as observed for the corresponding reaction of CNMe with $Cp^*_2Zr(CH_2SiMe_2CH_2)$.

Enamides **4** and **5** were identified by ^1H and ^{13}C NMR measurements. The protons of the characteristic exocyclic methylene group appear at δ 4.24 and 4.15 for **4** and at δ 4.58 and 4.54 for **5**. The gated nondecoupled ^{13}C NMR spectra of these compounds exhibit a doublet of doublets between 85 and 95 ppm confirming the presence of an exocyclic methylene group. The chemical shifts for the carbon and hydrogen atoms of the cyclopentadienyl rings, the methyl group bound to each nitrogen, and the silicon methyls have expected values. The carbon resonance of the remaining methylene group of the metallacyclic ring in **4** is observed as a triplet at δ 42.7 with $^1J_{C-H}$ = 120 Hz and is shifted slightly upfield from that observed for $Cp^*_2Zr(N(Me)C(=CH_2)SiMe_2CH_2)$.

The enamide complex **4** could not be prepared, however, without some contamination from the dienamide **5**. When the same reaction procedure for synthesizing **1** was used to prepare **4**, ^1H NMR measurements revealed a 50:50 mixture of **4** and **5**. However, by cooling the solution of $Cp_2Zr(CH_2SiMe_2CH_2)$ to –10 °C and then adding CNMe in small increments over a 7-day period, the relative ratio of **4** to **5** was eventually increased to 14:1. Apparently, the electrophilicity of **4** is sufficiently enhanced due to the replacement of Cp* by Cp that it can compete effectively with $Cp_2Zr(CH_2SiMe_2CH_2)$ for unreacted CNMe.

The reaction of excess CNMe with $Cp_2Zr(CH_2SiMe_2CH_2)$ at –20 °C, however, does not yield the corresponding enediamido complex. Under these conditions, a light orange solid precipitates out of the pentane

(41) Bocarsly, J. R.; Floriani, C.; Chiesa-Villa, A.; Guastini, C. *Organometallics* **1986**, *5*, 2380.
(42) (a) McMullen, A. K.; Rothwell, I. P.; Huffman, J. C. *J. Am. Chem. Soc.* **1985**, *107*, 1072. (b) Latesky, S. L.; McMullen, A. K.; Niccolai, G. P.; Rothwell, I. P.; Huffman, J. C. *Organometallics* **1985**, *4*, 1896. (c) Chamberlain, L. R.; Durfee, L. D.; Fanwick, P. E.; Kobriger, L. M.; Latesky, S. L.; McMullen, A. K.; Steffey, B. D.; Rothwell, I. P.; Folting, K.; Huffman, J. C. *J. Am. Chem. Soc.* **1987**, *109*, 6068. (d) Durfee, L. D.; McMullen, A. K.; Rothwell, I. P. *J. Am. Chem. Soc.* **1988**, *110*, 1463.
(43) Hessen, B.; Blenkers, J.; Teuben, J. H.; Helgesson, G.; Jagner, S. *Organometallics* **1989**, *8*, 830.
(44) Hofmann, P.; Frede, M.; Stauffert, P.; Lasser, W.; Thewalt, U. *Angew. Chem., Int. Ed. Engl.* **1985**, *24*, 712.

solution. Preliminary solution NMR measurements made at 25 °C of this solid indicate the presence of only one species.[45] Attempts to isolate and characterize this compound have been hindered by its tendency to rearrange in the solid state as well as in solution. Subsequent solution NMR measurements of the original product show at least three distinct products are formed at room temperature within 2 days. Isotopic labeling experiments will be undertaken in an effort to identify this intermediate and the corresponding rearrangement products.

Reaction of *tert*-Butyl Isocyanide with $Cp_2Zr(CH_2SiMe_2CH_2)$. Since the coordination environment about the zirconium in $Cp_2Zr(CH_2SiMe_2CH_2)$ is reasonably crowded, one might anticipate that steric factors could affect the course of the insertion chemistry. To investigate the steric influence of the alkyl substituent of the isocyanide, the reaction of *tert*-butyl isocyanide with $Cp_2Zr(CH_2SiMe_2CH_2)$ was investigated. ^1H NMR measurements indicate that this reaction proceeds at 25 °C with the initial consumption of 1 equiv of the isonitrile in 2 h. However, this insertion reaction is *not* accompanied by the occurrence of an intramolecular 1,2-silyl shift. Nucleophilic attack by *tert*-butyl isocyanide at the electrophilic Zr(IV) center is followed by its partial insertion into a zirconium–carbon bond of $Cp_2Zr(CH_2SiMe_2CH_2)$ and affords the η^2-iminoacyl zirconadicyclic complex $Cp_2Zr(N(CMe_3)CCH_2SiMe_2CH_2)$ (**6**) (eq 5). This compound has been

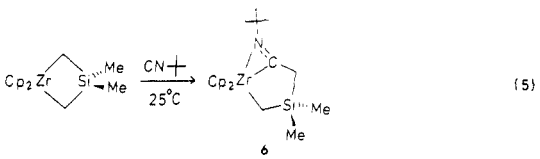

(5)

6

characterized by ^1H and ^{13}C NMR measurements, IR spectroscopy, and elemental analysis, and its molecular structure has been established by X-ray diffraction methods (vide infra).

The ^1H NMR resonances for the C_5H_5 ring, the *tert*-butyl substituent, and the dimethylsilyl group of **6** appear as singlets at δ 5.50, 1.07, and 0.19, respectively. Two different resonances are observed for the two methylene groups. The singlet at δ 2.51 is assigned to the methylene group attached to the carbon of the η^2-iminoacyl fragment, whereas the singlet at δ −0.11 is assigned to the methylene attached to Zr. In the corresponding gated nondecoupled ^{13}C NMR spectrum of **6**, the characteristic splitting patterns are observed for the ring carbons of C_5H_5, the methyl and quaternary carbons of the *tert*-butyl substituent, and the methyl carbons of the dimethylsilyl group at δ 106.6 (d, $^1J_{C-H}$ = 170 Hz), δ 29.7 (q, $^1J_{C-H}$ = 126 Hz) and 58.4 (s), and δ 2.3 (q, $^1J_{C-H}$ = 118 Hz), respectively. The methylene carbon attached to the carbon of the isocyanide is assigned to the triplet at δ 32.7 with $^1J_{C-H}$ = 125 Hz, whereas the methylene carbon which remains bound to zirconium is located at δ 5.8 with $^1J_{C-H}$ = 114 Hz. This latter assignment is compatible with the upfield location of the corresponding proton resonance. Finally, a low-intensity singlet is observed downfield at δ 232.5, consistent with the presence of an η^2-iminoacyl fragment in **6**.[46]

(45) This compound is characterized by several unusual spectral features. The ^1H NMR spectrum contains an AB quartet at δ 6.34 and 6.37 with J_{H-H} = 17.6 Hz and a singlet at δ −0.32; the gated nondecoupled spectrum exhibits a doublet of doublets centered at δ 141.8 with $^1J_{C-H}$ = 158.7 and 179.4 Hz.

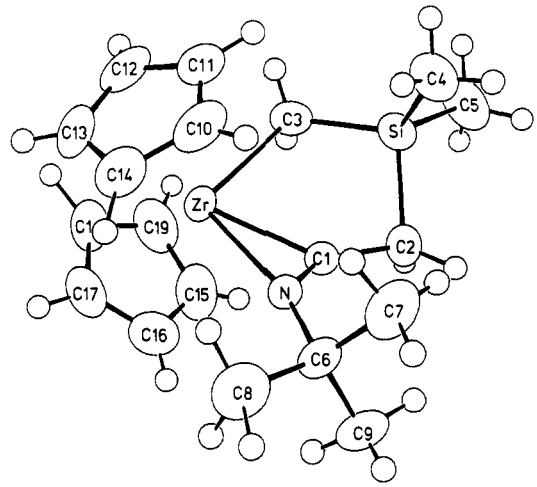

Figure 1. Perspective view of $Cp_2Zr(N(CMe_3)CCH_2SiMe_2CH_2)$ with appropriate numbering scheme. The thermal ellipsoids are scaled to 50% probability.

Further evidence supporting this mode of coordination is provided by the infrared spectrum which shows a carbon–nitrogen stretch at 1625 cm^{-1}. The corresponding stretching frequency of the carbon–nitrogen bond of an η^2-iminoacyl group unfortunately varies over a wide range from 1490 to 1760 cm^{-1}.[42a,46,47]

Description of the Molecular Structure of $Cp_2Zr(N(CMe_3)CCH_2SiMe_2CH_2)$. Although the spectroscopic data obtained for **6** provide compelling evidence supporting its structural formulation as an η^2-iminoacyl complex, an X-ray structure determination was undertaken to establish its molecular structure. The structural analysis of this zirconadicyclic complex confirms an "N-outside" conformation for the η^2-iminoacyl fragment. A perspective view of the molecular structure of **6** is shown in Figure 1 with the atom-labeling scheme. The compound crystallizes in a monoclinic crystal lattice of $P2_1/n$ symmetry with four discrete molecules per unit cell. The solid-state structure of **6** is well-behaved with no indication of disorder or excessive thermal motion.

The coordination environment about the zirconium atom consists of two π-bonded cyclopentadienyl rings, an η^2-iminoacyl fragment which is bonded in an "edge-on" fashion, and a methylene carbon. The partial insertion of *tert*-butyl isocyanide leads to the formation of two adjacent zirconacyclic rings of different size. The smaller three-membered ring containing Zr, C1, and N is characterized by an acute N–Zr–C1 bond angle of 33.2 (1)° and a Zr–N bond of 2.227 (3) Å which is noticeably longer than the Zr–C1 bond of 2.164 (4) Å. The C1–N bond of 1.255 (5) Å is comparable to that found in other η^2-iminoacyl complexes (see Table VII). The larger five-membered ring contains several interesting structural features that are worth noting. By sterically blocking the occurrence of the 1,2-silyl shift, the *tert*-butyl substituent has trapped the molecule in a structure that resembles a possible transition state for this intramolecular rearrangement. For example,

(46) (a) den Haan, K. H.; Luinstra, G. A.; Meetsma, A.; Teuben, J. H. *Organometallics* **1987**, *6*, 1509. (b) Bochmann, M.; Wilson, L. M.; Hursthouse, M. B.; Short, R. L. *Organometallics* **1987**, *6*, 2556 and references cited therein. (c) Erker, G.; Korek, U.; Petersen, J. L. *J. Organomet. Chem.* **1988**, *355*, 121 and references cited therein.

(47) Bellachioma, G.; Cardaci, G.; Zanazzi, P. *Inorg. Chem.* **1987**, *26*, 84.

(48) Reger, D. L.; Tarquini, M. E.; Lebioda, L. *Organometallics* **1983**, *2*, 1763.

Table VII. Bond Angles and Distances of η^2-Iminoacyl Zr(IV) Complexes

compound	N–Zr–C, deg	Zr–C, Å	Zr–N, Å	C–N, Å	ref
$Cp_2Zr(Ph)[\eta^2\text{-}N(CH_2Ph)C{=}CHPPh_3]$	34.6 (2)	2.249 (4)	2.148 (4)	1.312 (6)	46c
$Zr(OAr')_2[\eta^2\text{-}N(CMe_3)C{-}CH_2Ph]_2$	33.6	2.228 (3)	2.221 (3)	1.286 (4)	42b
$[HB(3,5\text{-}Me_2pz)_3]Zr(O\text{-}t\text{-}Bu)(\eta^2\text{-}N(CMe_3)CMe)Me$	33.6 (4)	2.20 (11)	2.194 (8)	1.27 (2)	48
$Cp_2Zr(N(CMe_3)CCH_2SiMe_2CH_2)$ (**6**)	33.2 (1)	2.164 (4)	2.227 (3)	1.255 (5)	this work
$Cp_2Zr(N(CMe_3)C{-}C(=NCMe_3)CH_2SiMe_2CH_2)$ (**7**)	33.1 (1)	2.216 (4)	2.231 (3)	1.266 (4)	this work

the long Si–C2 bond of 1.907 (5) Å and the reduced C1–C2–Si angle of 97.4 (3)° presumably reflect initial structural changes that precede the breaking of the Si–C2 bond and the subsequent formation of the exocyclic methylene group. The Zr–C3(methylene) bond of 2.396 (6) Å is ca. 0.15 Å longer than the corresponding zirconium–carbon bond of 2.240 (5) Å in the parent metallacycle $Cp_2Zr(CH_2SiMe_2CH_2)$.[49] The lengthening of this bond is a consequence of the η^2-iminoacyl fragment, which occupies two of the three frontier orbitals of the canted zirconocene fragment.[27] This interaction reduces the acceptor ability of the remaining metal orbital and leads to an elongation of this zirconium–carbon bond in **6**. The analogous structural effect is observed for $Cp_2Zr(Ph)[\eta^2\text{-}N(CH_2Ph)C{=}CHPPh_3]$[46c] in which the Zr–C(Ph) = 2.389 (5) Å.

The fact that C1 remains bound to zirconium in this η^2-iminoacyl complex is particularly significant in light of the theoretical calculations performed by Hoffmann and co-workers[15] on related η^2-acyl species. For a "carbenium-like" transition state the zirconium–carbon bond should remain intact. More importantly, if this description is reasonable, then the corresponding carbon center, C1, in $Cp_2Zr(N(CMe_3)CCH_2SiMe_2CH_2)$ should be susceptible to nucleophilic attack. Chemical evidence for this behavior is provided by the reaction of **6** with a second equivalent of *tert*-butyl isocyanide.

Reaction of $Cp_2Zr(N(CMe_3)CCH_2SiMe_2CH_2)$ with *tert*-Butyl Isocyanide. The addition of a second equivalent of *tert*-butyl isocyanide to **6**, as monitored by periodic NMR measurements, is complete in 5 days at 25 °C. In this case, despite the abnormally long Zr–C3 bond of 2.396 (6) Å in **6**, the *tert*-butyl isocyanide does not insert into this bond. This result is not surprising since the zirconium center of **6** is coordinatively saturated. Lateral attack of the Zr from the other side is further blocked by the *tert*-butyl group. Consequently, the insertion of the second molecule of CN-*t*-Bu probably proceeds by nucleophilic attack at the more accessible carbon, C1, of the η^2-iminoacyl group and results in the reductive coupling of two molecules of CN-*t*-Bu and the formation of $Cp_2Zr(N(CMe_3)C{-}C(=NCMe_3)CH_2SiMe_2CH_2)$ (**7**). This second insertion step presumably involves transfer of the "carbenium-like" center to the carbon of the coordinated isonitrile followed by a 1,2-methylene shift (eq 6). This

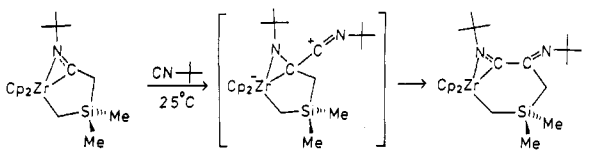

6 7 (6)

(49) Tikkanen, W. R.; Egan, J. W., Jr.; Petersen, J. L. *Organometallics* **1984**, *3*, 1646.

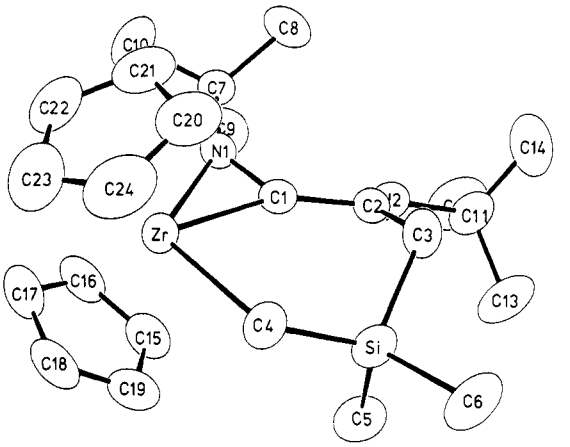

Figure 2. Perspective view of $Cp_2Zr(N(CMe_3)C{-}C(=NCMe_3)CH_2SiMe_2CH_2)$ with appropriate numbering scheme. The thermal ellipsoids are scaled to 50% probability. The hydrogen atoms have been omitted for clarity.

unusual η^2-iminoacyl compound was characterized by ^1H and ^{13}C NMR measurements, IR spectroscopy, elemental analysis, and a single-crystal X-ray structure determination.

In the ^1H NMR spectrum two different resonances are observed at δ 1.33 and 1.37 for the protons of the *tert*-butyl groups, consistent with two different chemical environments. The corresponding methyl and quaternary carbon resonances of the two inequivalent *tert*-butyl groups are centered at δ 29.7, 31.1 and δ 55.7, 61.4, respectively. The observation of a singlet at δ −0.44 confirms that a methylene remains bound to the zirconium atom in a manner similar to that observed in **6**. Finally, the ^{13}C resonance at δ 228.9 is characteristic of an η^2-iminoacyl fragment. The ^{13}C chemical shift of the carbon of the second isonitrile bound to the carbon of the η^2-iminoacyl unit is at δ 169.3. The remaining ^1H and ^{13}C NMR resonances for the cyclopentadienyl rings, the other methylene, and the dimethylsilyl group are easily assignable on the basis of their chemical shifts and splitting patterns. Consistent with the NMR data, two different carbon–nitrogen stretches are observed in the IR spectrum of **7**. The main band is centered at 1595 cm^{-1} with a shoulder at 1605 cm^{-1}.

Description of the Molecular Structure of $Cp_2Zr(N(CMe_3)C{-}C(=NCMe_3)CH_2SiMe_2CH_2)$. The molecular structure of **7** has been confirmed by X-ray crystallography. A perspective view of its molecular configuration is displayed in Figure 2 with the appropriate atom labeling scheme. The analysis reveals that the "N-outside" conformation of the η^2-iminoacyl fragment originally observed for **6** is retained. The insertion of the second molecule of *tert*-butyl isocyanide proceeds with the formation of a new carbon–carbon single bond with C1–C2 = 1.492 (5) Å and the expansion of the five-membered ring of **6** to a six-membered metallacyclic ring. A comparison of the pertinent structural parameters provided in Tables

V and VI for the respective zirconadicyclic rings of **6** and **7** shows that this expansion of the larger zirconacyclic ring is accompanied by a 10° increase in the C–Zr–C bond angle and a 0.05 Å lengthening of the Zr–C1 bond common to both rings. These structural changes produce a more symmetrical arrangement of the substituents of the η^2-iminoacyl group. The carbon–nitrogen bond distances of the exocyclic imine (C2–N2 = 1.259 (5) Å) and the η^2-iminoacyl (C1–N1 = 1.266 (4) Å) are essentially equivalent, within experimental error. As expected, the Zr–C4 (methylene) bond of 2.378 (4) Å remains long. Finally, the orientation of the two *tert*-butyl groups minimizes steric repulsions between these bulky substituents.

Concluding Remarks

The results of our investigation of the zirconium-induced insertion of CNR into the Zr bond(s) of $Cp_2\overline{Zr(CH_2SiMe_2CH_2)}$ reveal that the course of this reaction is significantly influenced by substituent effects. At 25 °C, lateral insertion of CNMe is followed by an intramolecular 1,2-silyl shift producing the cyclic eneamide **4**. Alternatively for CN-*t*-Bu, the corresponding η^2-iminoacyl intermediate is sterically trapped as **6**. The molecular structure of **6** is compatible with that expected for an η^2-"carbenium-like" species with the carbon remaining bound to Zr without any noticeable lengthening of the C–N bond. More importantly, the η^2-iminoacyl carbon of **6** is sufficiently electrophilic to permit nucleophilic attack by a second molecule of CN-*t*-Bu leading to the reductively coupled product **7**. This result is particularly significant since it provides by analogy direct chemical evidence of Hoffmann's alternative view[15] for the reactivity associated with an electrophilic η^2-iminoacyl group.

The molecular structure of **7** is particularly intriguing since it may structurally resemble the reactive intermediate involved in the reductive-coupling reaction that leads to the formation of a bicyclic enediamidate, such as **3** (eq 3). Thermolysis experiments[50] in fact show that **7** rearranges at 120 °C ($t_{1/2}$ = 2.9 min) to one product, which on the basis of the spectral and analytical data[51] is the corresponding enediamidate complex $Cp_2\overline{Zr(N(CMe_3)C(CH_2SiMe_2CH_2)=CN(CMe_3))}$ (**8**). This rearrangement

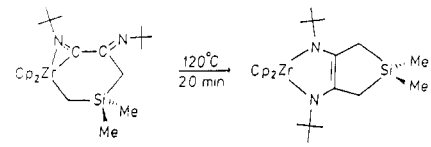

(7)

7 **8**

presumably is initiated by an intramolecular 1,2-shift of the Zr-bound methylene to the electrophilic carbon of the η^2-iminoacyl group in **7**. Further studies are underway to investigate the mechanistic implications of this unusual rearrangement to our understanding of the reductive-coupling process.

Acknowledgment. Support for this research was provided by the donors of the Petroleum Research Fund, administered by the American Chemical Society. J.L.P. further expresses his appreciation to Professor John Bercaw for helpful suggestions. Computer time for the X-ray structural analyses was provided by the West Virginia Network for Educational Telecomputing.

Registry No. **1**, 122236-17-3; **2**, 122236-18-4; **3**, 122236-19-5; **4**, 122236-20-8; **5**, 122236-21-9; **6**, 122236-22-0; **7**, 122236-23-1; **8**, 122236-24-2; $Cp^*_2\overline{Zr(CH_2SiMe_2CH_2)}$, 109996-91-0; CNMe, 593-75-9; $Cp_2\overline{Zr(CH_2SiMe_2CH_2)}$, 89530-31-4; CN-*t*-Bu, 7188-38-7.

Supplementary Material Available: Tables of thermal parameters, all non-hydrogen bond distances and angles, and pertinent least-squares planes for **6** and **7** (13 pages); listings of observed and calculated structure factors for **6** and **7** (23 pages). Ordering information is given on any current masthead page.

(50) Berg, F. J.; Petersen, J. L., work in progress.

(51) $Cp_2\overline{Zr(N(CMe_3)C(CH_2SiMe_2CH_2)=CN(CMe_3))}$: ^{1}H NMR spectrum ($C_6D_6$) δ 6.06, 5.37 ($C_5H_5$, s), 1.39 ($NCCH_3$, s), 2.01, 1.20 ($C{=}CH_2$, dd, J_{H-H} = 16.9[52]), 0.21, 0.16 ($SiCH_3$, s); gated nondecoupled ^{13}C NMR spectrum (mult, $^1J_{C-H}$ in Hz) δ 122.3 ($NC{=}$, s), 108.2, 103.1 (C_5H_5, d, 170), 58.6 ($NCCH_3$, s), 34.4 ($NCCH_3$, q, 125), 22.4 ($=CCH_2$, t, 123), −2.21, −2.84 ($SiCH_3$, q, 118); λ_{max} = 352 nm. Anal. Calcd for $C_{24}H_{38}N_2SiZr$: C, 60.83; H, 8.08; N, 5.91. Found: C, 60.11; H, 8.08; N, 5.40 (ORS).

(52) The methylene protons appear as an AB quartet with a geminal coupling of 16.9 Hz. The inequivalence of their chemical environments arises from a significant folding along the N···N vector of the five-membered ZrN_2C_2 ring. This deviation from planarity causes the two Cp rings and the two methyl groups of $SiMe_2$ to be inequivalent.[41]